

RESEARCH ARTICLE | JANUARY 02 2024

Solvent-mediated modification of thermodynamics and kinetics of monoethanolamine regeneration reaction in amine-stripping carbon capture: Computational chemistry study

N. D. Afify   ; M. B. Sweatman 

 Check for updates

J. Chem. Phys. 160, 014501 (2024)

<https://doi.org/10.1063/5.0169382>


View
Online


Export
Citation

Articles You May Be Interested In

Molecular dynamics simulation of microwave heating of liquid monoethanolamine (MEA): An evaluation of existing force fields

J. Chem. Phys. (May 2018)

Evaluation of porosity and pressure drop on kenaf-monoethanolamine (MEA) modified sorbent for carbon dioxide adsorption application

AIP Conf. Proc. (December 2023)

Improvement of carbon dioxide adsorption by the effect of concentration on blended amine-kenaf impregnation in IsoSORP analyzer

AIP Conf. Proc. (July 2023)

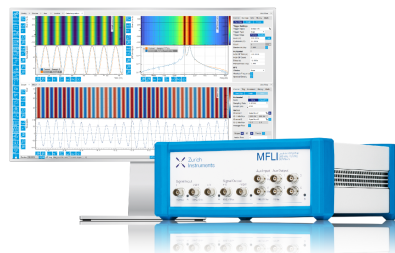
Challenge us.

What are your needs for periodic signal detection?



Zurich
Instruments

[Find out more](#)



Solvent-mediated modification of thermodynamics and kinetics of monoethanolamine regeneration reaction in amine-stripping carbon capture: Computational chemistry study

Cite as: J. Chem. Phys. 160, 014501 (2024); doi: [10.1063/5.0169382](https://doi.org/10.1063/5.0169382)

Submitted: 25 July 2023 • Accepted: 22 November 2023 •

Published Online: 2 January 2024



[View Online](#)



[Export Citation](#)



[CrossMark](#)

N. D. Afify^{a)} and M. B. Sweatman

AFFILIATIONS

Institute for Materials and Processes, School of Engineering, The University of Edinburgh, Edinburgh EH9 3FB, United Kingdom

^{a)}Author to whom correspondence should be addressed: N.Afify@ed.ac.uk

ABSTRACT

A major limitation of amine-based post-combustion carbon capture technology is the necessity to regenerate amines at high temperatures, which dramatically increases operating costs. This paper concludes the effect of solvent choice as a possible route to modify the thermodynamics and kinetics characterizing the involved amine regeneration reactions and discusses whether these modifications can be economically beneficial. We report experimentally benchmarked computational chemistry calculations of monoethanolamine regeneration reactions employing aqueous and non-aqueous solvents with a wide range of dielectric constants. Unlike previous studies, our improved computational chemistry framework could accurately reproduce the right experimental activation energy of zwitterion formation. From the thermodynamics and kinetics of the predicted reactions, the use of non-aqueous solvents with small dielectric constants led to reductions in regeneration Gibbs free energies, activation barriers, and enthalpy changes. This can reduce energy consumption and give an opportunity to run desorption columns at relatively lower temperatures, thus offering the possibility of relying on low-grade waste heat as an energy input.

© 2024 Author(s). All article content, except where otherwise noted, is licensed under a Creative Commons Attribution (CC BY) license (<http://creativecommons.org/licenses/by/4.0/>). <https://doi.org/10.1063/5.0169382>

15 October 2024 09:30:19

I. INTRODUCTION

Amine-based post-combustion carbon capture (PCCC) technology is currently one of the most mature routes in the world fight against climate change.¹ This technology involves a continuous cyclic process of CO₂ molecules' absorption and desorption by an amine.^{2,3} An exhaust gas containing CO₂ passes through the bottom of an absorption column, where it comes into contact with an amine solution. The CO₂ molecules then react with amine molecules, forming carbamate at temperatures ranging from 40 to 60 °C at atmospheric pressure.^{2,3} The CO₂-rich amine solution then flows to a stripping column, where it undergoes an endothermic regeneration reaction to reproduce the spent amine and a purified CO₂ stream for storage. The remaining amine-rich solution then

exits the bottom of the stripping column and recirculates back to the absorption column for the next cycle.

The above amine-based PCCC technology suffers from high operating energy costs, since it requires regenerating the spent amine at high temperatures, typically between 120 and 140 °C at 1–2 bar.^{2,4–7} Reduction of these energy costs has become an important research area.^{2–8} In the past few years, researchers followed several approaches to reduce such large energy costs. One approach was to replace conventional steam heating by microwave heating^{2,9–11} or frequency-tuned infrared preferential heating¹² of amine solutions. Another research approach used different amine types,^{13–18} including monoethanolamine (MEA), diethanolamine (DEA), triethanolamine (TEA), diisopropanolamine (DIPA), 2-amino-2-methyl-1-propanol (AMP), and methyldiethanolamine

(MDEA). A third research direction to reduce amine regeneration energy consumption focused on the evaluation of several aqueous^{19–22} and non-aqueous solvents.^{23–30}

In this computational work, we are interested in understanding if the use of non-aqueous solvents with small dielectric constants can lead to amine regeneration processes with less energy consumption or lower regeneration temperature requirements when compared to the use of water as a solvent. Our study selected monoethanolamine (MEA) as it is the most industrially used amine.¹¹ To obtain a clear picture of the role of solvent, we studied several solvents with a wide range of static dielectric constants, ranging from 7.43 up to 108.94 at room temperature. Our solvents included tetrahydrofuran (THF), t-butanol, 1-pentanol, acetone, ethanol, methanol, dimethyl sulfoxide (DMSO), water, and formamide.

II. COMPUTATIONAL DETAILS

Although our initial testing simulations were carried out using the GAUSSIAN 16³¹ and General Atomic and Molecular Electronic Structure System GAMESS³² codes, for performance reasons, our

production calculations were fully carried out using the ORCA 5.0.3 code.³³ Our computational work was carried out on the Cirrus and Eddie high-performance computing clusters available at the University of Edinburgh. Before looking into the effect of solvent choice on the thermodynamics and kinetics of involved amine regeneration reactions, it was very important to benchmark the accuracy of our computational chemistry calculations against experimental data. This was carried out through a comprehensive testing of the mechanisms and kinetics characterizing the CO₂ reaction with MEA in the presence of water as a solvent.

While geometry optimization, intrinsic reaction coordinate (IRC),³³ and frequency calculations were carried out using density function theory (DFT), final single-point electronic energies were computed using the domain-based local pair natural orbital coupled-cluster method DLPNO-CCSD(T)^{33,34} implemented in the ORCA code. In all calculations, implicit solvent effects were included using the polarizable continuum model (PCM)³⁵ in conjunction with the Pauling atomic radii.³⁶ The Def2-TZVP basis set³³ was employed in both DFT and DLPNO-CCSD(T) calculations. To reach the most accurate computational framework, we evaluated

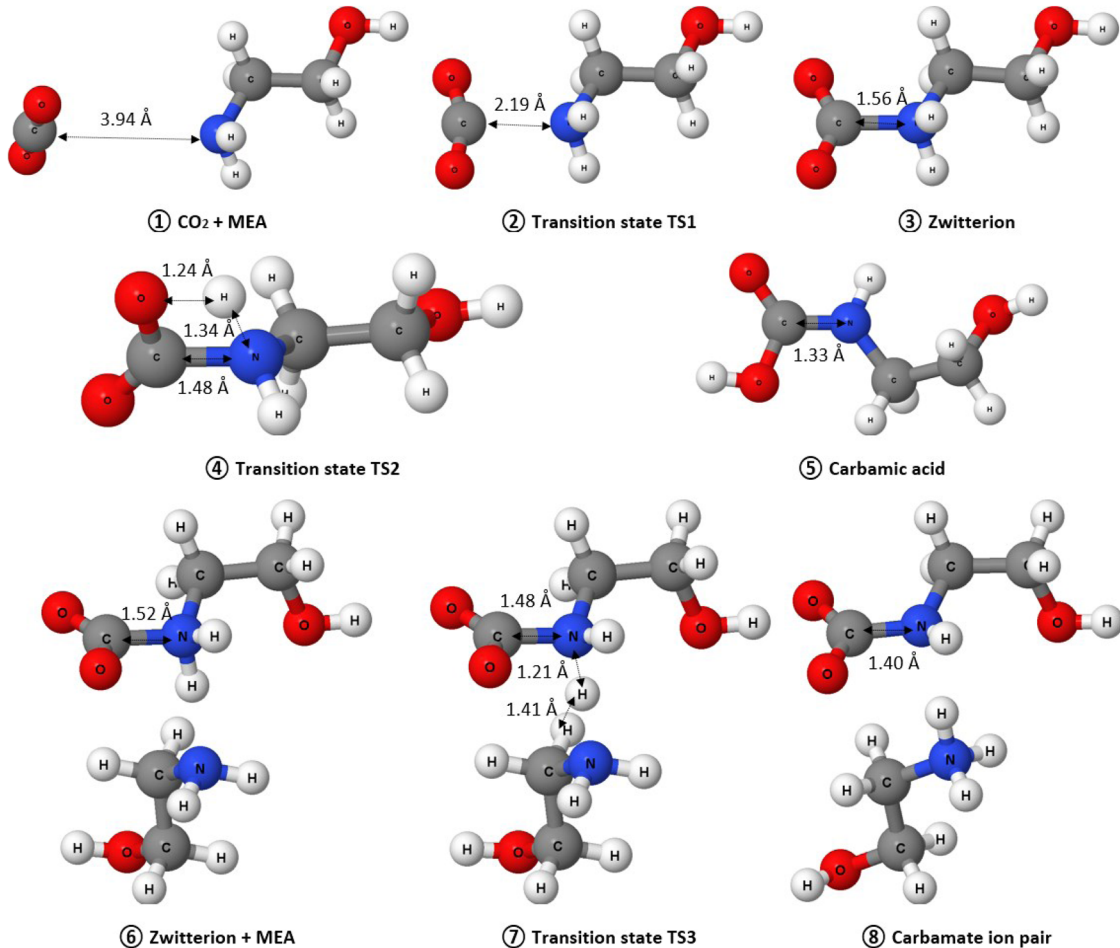


FIG. 1. DFT optimized molecular geometries of reactants, products, and transition states involved in the reaction of CO₂ with MEA in the presence of water as a solvent. Reported geometries correspond to the TPSS0/Def2-TZVP level of theory.

several DFT functionals. Although most of the previous computational studies^{36–46} were carried out using the most commonly used B3LYP hybrid functional, the B3LYP functional has recently turned out to be of average performance when it comes to thermochemistry⁴⁷ calculations.⁴⁸ In addition to B3LYP, we tested several meta-GGA and hybrid meta-GGA functionals, including TPSS, TPSSh, TPSS0, M06, M062X, M06L, rM06L, and SCANfunc, and range-separated hybrid functionals, including wB97, wB97X, wB97X-D3, wB97X-D4, wB97X-D3BJ, and CAM-B3LYP.³³ Gibbs free energies, activation barriers, and enthalpy changes were calculated by combining the DLPNO-CCSD(T) electronic energies and DFT vibrational analysis results.

Our DFT calculations included the zero-point energy and geometrical counterpoise corrections.⁴⁹ We have also evaluated the effect of including Grimme's dispersion correction (D3BJ version).⁵⁰ As it will be discussed later, the current chemical reactions including the dispersion correction caused more deviation from experimental activation energies. Therefore, we have decided to proceed only with the geometrical counterpoise correction since it produces the best agreement with experimental activation energies.

III. RESULTS AND DISCUSSION

A. Accuracy of thermochemistry predictions

In this section, we evaluate the accuracy of our computational framework in reproducing the correct reaction mechanisms and experimental activation energy in the case of water as a solvent. In agreement with all previous computational studies,^{36–46} all evaluated DFT functionals have predicted the same reaction mechanisms. In Fig. 1, we report the DFT-optimized molecular geometries in the major reaction steps in the case of the TPSS0 functional. Relative electronic energies corresponding to these geometries are shown in the potential energy surface reported in Fig. 2.

We first discuss the possible reaction mechanisms. From steps 1, 2, and 3 in Fig. 1, we can see that one CO₂ molecule reacts with one MEA molecule to form zwitterion. This zwitterion can then enter one of the following two routes. The first possibility is the formation of carbamic acid (steps 3, 4, and 5). The second possibility is the

reaction of zwitterion with a nearby MEA molecule to form carbamate ion pairs (steps 6, 7, and 8). From the potential energy surface reported in Fig. 2, we can confirm that the formation of carbamic acid is energetically unfavorable in agreement with previous studies. In summary, the main reaction steps involved in amine-based carbon capture are the formation of zwitterion and the subsequent formation of carbamate ion pairs. This mechanism agrees well with several computational studies.^{36–46}

In Table I, we report the activation energies for zwitterion and carbamate formation (i.e., forward reactions) and regeneration (i.e., backward reactions). These activation energies were obtained by combining the DLPNO-CCSD(T) electronic energies and DFT frequency calculations at 298.15 K and 1 bar. In Table S1 (supplementary material), we compare these values to activation energies calculated purely from DFT electronic energies and frequency calculations. Table S1 also contains the activation energies for the unfavorable carbamic acid reaction route. At this point, it is important to decide which DFT functional produces the most accurate results. Experimental activation energies for zwitterion formation were reported by Ali⁵¹ (11.14 kcal/mol) and Alper⁵² (11.16 kcal/mol) using the direct stopped-flow technique. From Table I, it is clear that the TPSS0 was the best DFT functional able to accurately predict the experimental activation energy of zwitterion formation.

In the following, we give an additional reason why the above result is indeed important. Some previous computational chemistry studies compared their predicted activation energies for zwitterion formation to the above experimental studies.^{36–39} Unfortunately, authors in these studies compared their predicted activation energies to the wrong experimental value, namely, 12.4 kcal/mol. The used experimental activation energy in fact corresponds to the case of the AMP amine, not MEA.^{51,53} This point was very important to comment on in order to avoid potential confusion in future studies.

TABLE I. Activation energies (kcal/mol) obtained by combining the DFT frequency calculations at 298.15 K and DLPNO-CCSD(T) electronic energies. All calculations used water as a solvent and employed the Def2-TZVP basis set. Boldface denotes the most accurate functional and activation energies with respect to available experimental data.

	Zwitterion		Carbamate	
	Forward	Backward	Forward	Backward
B3LYP	9.97	5.09	0.13	6.71
TPSS	8.19	4.20	0.10	6.39
TPSSh	10.80	4.56	-0.04	6.67
TPSS0	11.13	4.74	-0.22	6.96
M06	8.10	5.61	0.81	5.35
M062X	7.14	4.86	0.08	4.87
M06L	7.79	5.37	-0.97	5.86
rM06L	8.86	5.36	-0.72	6.96
SCANfunc	6.36	3.65	-1.27	5.30
wB97	8.17	5.00	0.79	5.47
wB97X	8.57	4.93	0.07	5.77
wB97X-D3	9.71	4.93	0.06	5.50
wB97X-D4	8.83	4.87	-0.08	5.57
wB97X-D3BJ	8.86	4.81	-0.20	5.61
CAM-B3LYP	9.48	4.84	-0.19	5.70

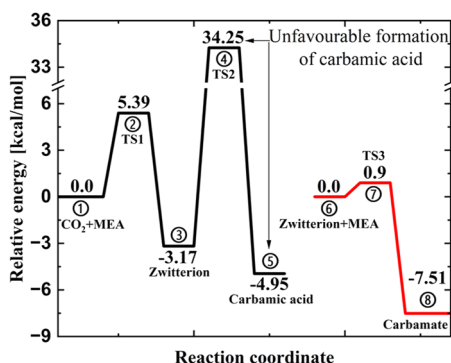


FIG. 2. Relative potential energy surface corresponding to the molecular geometries reported in Fig. 1. Reported values correspond to single-point electronic energies computed at the DLPNO-CCSD(T)/Def2-TZVP level of theory.

As mentioned above in Sec. II, our DFT calculations evaluated the effects of including the geometrical counterpoise⁴⁹ and Grimme's dispersion⁵⁰ corrections. In the following, we justify our decision to consider results obtained by incorporating only the geometrical counterpoise correction. In Table S3 (supplementary material), we report the effect of including these two corrections on the zwitterion formation activation energy. Results are reported for the case of water as a solvent and B3LYP, TPSS, TPSSh, and TPSS0 DFT functionals. In this table, ΔE_{exp} represents the deviation of the calculated activation energy from the experimental value (11.15 kcal/mol). Inspection of the results reported in Table S3 reveals the following four cases.

Let us first discard both the counterpoise and dispersion corrections. In this case, the TPSS0 functional produces the best agreement with the experimental activation energy ($\Delta E_{\text{exp}} = 0.46$ kcal/mol), followed by TPSSh ($\Delta E_{\text{exp}} = 0.76$ kcal/mol) and B3LYP ($\Delta E_{\text{exp}} = 1.61$ kcal/mol). In the second case, we included both the counterpoise and dispersion corrections. This makes B3LYP the most accurate functional ($\Delta E_{\text{exp}} = 1.68$ kcal/mol), followed by TPSSh ($\Delta E_{\text{exp}} = 2.24$ kcal/mol) and TPSS ($\Delta E_{\text{exp}} = 2.76$ kcal/mol). In the third case, we included only the dispersion correction. In this case, again the B3LYP functional comes the best ($\Delta E_{\text{exp}} = 1.68$ kcal/mol), followed by TPSS ($\Delta E_{\text{exp}} = 2.03$ kcal/mol) and TPSS0 ($\Delta E_{\text{exp}} = 2.54$ kcal/mol). In the fourth case, we included only the counterpoise correction. This puts the TPSS0 functional as the absolute best ($\Delta E_{\text{exp}} = 0.02$ kcal/mol) functional, followed by the TPSSh ($\Delta E_{\text{exp}} = 0.35$ kcal/mol) and B3LYP ($\Delta E_{\text{exp}} = 1.18$ kcal/mol) functionals.

The above analysis reveals the sensitivity of the obtained activation energies to the employed DFT functional and inclusion of dispersion and counterpoise corrections. In this study, we were looking for the best computational framework able to produce the best agreement with experimental data. Given the results of the above analysis, we believe the use of the TPSS0 functional in conjunction with the counterpoise corrections is effectively the best choice for studying the current chemical reactions. This is consistent

with a recent computational chemistry study,⁵⁴ which showed that the hybrid B3LYP functional, having 20% HF exchange, presented a poor performance compared to hybrid meta-GGA functionals having 25% HF exchange.

B. Effect of solvent choice on regeneration thermodynamics and kinetics

In this section, we comment on the effect of solvent choice on the thermodynamics and kinetics of amine regeneration reactions. As discussed above, the regeneration reaction consists of two main steps. The first step involves two amine molecules, where carbamate anion abstracts one proton from another protonated amine molecule, resulting in zwitterion and neutral amine molecules. The second step is the liberation of CO₂ molecules from zwitterion, resulting in unreacted CO₂ and amine molecules. In Table II, we report the Gibbs free energies and activation energy barriers corresponding to these two steps, in addition to the total regeneration enthalpy change. In Table II, we also report experimental specific heat capacities of the different solvents, taken from the Springer Materials database.

First, we discuss the dependence of reaction thermodynamics on the solvent type. From the computed Gibbs free energies, we can see that the regeneration of zwitterion from carbamate (first step) is an endothermic reaction. On the contrary, the regeneration of amine from zwitterion (second step) is a spontaneous reaction, as evidenced from the negative Gibbs free energy. From the enthalpy changes reported in Table II, it is very clear that using non-aqueous solutions with small dielectric constants can reduce the amount of input energy required to achieve the amine regeneration reaction. It is important to point out that the reduction in the required energy input cannot be explained only by the differences in specific heat capacities reported in Table II. For example, the use of formamide would require more energy input than water although formamide has almost half of the heat capacity of water.

This finding agrees well with a recent experimental study.⁸ In this study, Bougie *et al.* studied several solvents including a mixture

TABLE II. Effect of solvent choice on thermodynamics and kinetics of amine regeneration reactions. These results were obtained by combining the DFT frequency calculations at 298.15 K and DLPNO-CCSD(T) electronic energies. DFT calculations were carried out at the TPSS0/Def2-TZVP level of theory.

Solvent	Dielectric constant	Step 1: Carbamate to zwitterion		Step 2: Zwitterion to MEA		Enthalpy change (kcal/mol)	Specific heat capacity (J/gK)
		Gibbs free energy (kcal/mol)	Activation energy (kcal/mol)	Gibbs free energy (kcal/mol)	Activation energy (kcal/mol)		
THF	7.43	2.38	3.20	-7.77	1.95	0.43	1.770
t-butanol	12.47	4.18	4.46	-5.94	3.05	3.47	2.359
1-Pentanol	15.13	4.67	4.81	-7.98	3.38	4.90	2.336
Acetone	20.49	5.35	5.36	-7.70	3.79	5.96	2.131
Ethanol	24.85	5.75	5.70	-7.19	4.01	6.49	2.512
Methanol	32.61	6.26	6.14	-4.76	4.25	6.48	2.508
DMSO	46.83	7.00	6.82	-6.62	4.50	7.68	1.960
Water	78.36	7.18	6.96	-6.39	4.74	8.22	4.188
Formamide	108.94	7.09	6.85	-6.20	4.82	8.45	2.388

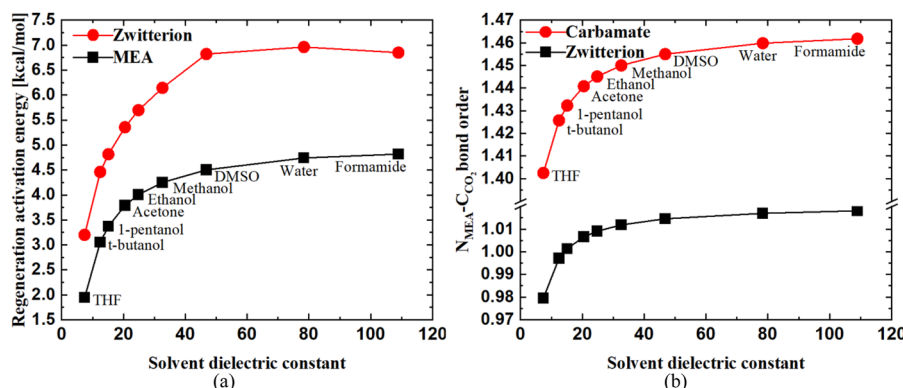


FIG. 3. (a) Effect of the solvent dielectric properties on the activation energies of the two regeneration reaction steps. Red circles and black squares correspond to converting carbamate into zwitterion and zwitterion into MEA. (b) Relative chemical stabilities of zwitterion and carbamate as calculated from bond order analysis of the $N_{MEA}-C_{CO_2}$ bond.

of ethylene glycol and 1-propanol, diethylene glycol monoethyl ether (DEGMEE), and N-methylformamide (NMF). They found that energy consumption reduces from 3630 kJ/mol in the case of water (dielectric constants of 78.355) to 929 kJ/mol in the case of DEGMEE (dielectric constant of 12.6). The findings in this experimental study fully support our computational results.

Now, we focus on the effect of solvent choice on the kinetics of the regeneration reaction. Activation energies for the two regeneration steps are reported in Table II. Figure 3(a) shows the dependence of these activation energies on the solvent dielectric constant. As we can see, the regeneration of zwitterion from carbamate exhibits higher activation energies compared to the regeneration of MEA from zwitterion. This indicates that the regeneration of zwitterion from carbamate is the rate-determining regeneration step regardless of the employed solvent. Going from formamide to THF, we can see that the activation energy decreases as a function of the solvent dielectric constant.

To confirm the dependence of activation energy on the solvent, in Fig. 3(b), we report the bond order analysis of the $N_{MEA}-C_{CO_2}$ bonds in zwitterion and carbamate. This bond order analysis gives us an idea about the relative chemical stabilities of zwitterion and carbamate. The bond order analysis was carried out using the Löwdin population analysis⁵⁴ implemented in the ORCA code.³³ From Fig. 3(b), it can be understood that the $N_{MEA}-C_{CO_2}$ bond in zwitterion is covalent in nature and becomes relatively weaker when we use solvents with a small dielectric constant. The $N_{MEA}-C_{CO_2}$ bond in carbamate has values between 1.4 and 1.46, depending on the employed solvent, which suggests that it is a partially ionic bond. Thus, the $N_{MEA}-C_{CO_2}$ bond in carbamate is much stronger than that in zwitterion, which explains why zwitterion regeneration is the rate-determining step, which is indeed documented in Fig. 3(a).

In the following, we seek to understand how the reduction in regeneration activation energy reported in Table II and Fig. 3(a) will play out in terms of heat input requirements. Higher activation energy implies that the solution should be heated at a higher temperature; thus, molecules will have sufficient energy to cross the energy barrier. Lowering this temperature will lower the rate at which carbamate decomposed into amine and CO_2 . The fact that non-aqueous

solutions with low dielectric constants exhibit lower activation energies means that amines can be regenerated in these solutions at lower temperatures compared to aqueous solutions, assuming the same amine regeneration rate.

In Fig. 4, we report the amine regeneration rate constant as a function of temperature for the different solvents. The MEA regeneration reaction rate constants were calculated using the Eyring equation.³⁴ From this figure, the regeneration reaction rate at any regeneration temperature increases by decreasing the solvent dielectric constant. This agrees well with the recent experimental results obtained by Bougie *et al.*⁸ In this experimental study, it was found that the amount of desorbed CO_2 in the case of the DEGMEE solvent (dielectric constant of 12.6) was much higher than in the case of water (dielectric constant of 78.4). Similarly, the amount of desorbed CO_2 in the case of water was much higher than in the case of the NMF solvent (dielectric constant of 182.0). Thus, our computational regeneration kinetics results are in line with those obtained experimentally.⁸

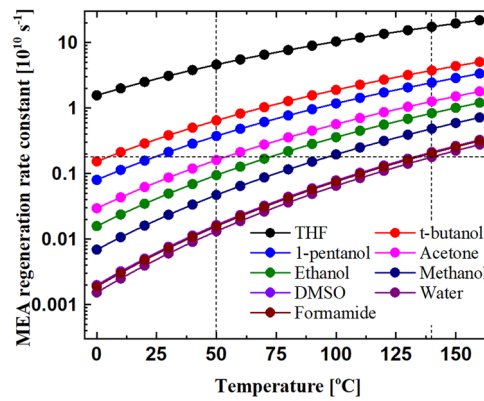


FIG. 4. MEA regeneration reaction rate constant as a function of temperature and solvent dielectric constant.

Taking into account that typical regeneration temperature in the case of water is about 140 °C,^{2,4–7} we can now estimate from Fig. 4 what regeneration temperatures are required for other solvents, keeping the same regeneration rate constant. From this figure (see dashed lines), it is possible to achieve MEA regeneration reaction at much lower temperatures if we use solvents with low dielectric constants. For example, in the case of acetone as a solvent, the regeneration temperature would be as low as 50 °C, which is much less than the 140 °C required in the case of water.

The solvent vapor pressure is a very important factor to consider when judging the suitability of a certain solvent for carbon capture applications. Acetone, for example, has a vapor pressure of 30.6 kPa at 25 °C, which is much higher than the vapor pressure of water (3.2 kPa at 25 °C). From this point of view, acetone might not be a suitable solvent. Our results show that the required amine regeneration temperatures can be significantly reduced by using non-aqueous solutions with small dielectric constants. However, it is important to look for a solvent with a small dielectric constant as well as low vapor pressure. One interesting solvent could be diethylene glycol monoethyl ether (DEGMEE), which has a dielectric constant of 12.6, which is very close to t-butanol included in our study. DEGMEE has a vapor pressure of 0.02 kPa, which makes it a very good candidate. This explains why DEGMEE was ranked as the best solvent in the recent experimental study conducted by Bougie *et al.*⁸

IV. CONCLUSION

In this computational study, we investigated the possibility of using non-aqueous solutions to reduce the energy penalty of amine regeneration in amine-based post-combustion carbon capture (PCCC) technology. We demonstrated the ability of our computational framework to reproduce very well the experimental activation energy of zwitterion formation. We have shown that non-aqueous solutions with small dielectric constants are beneficial for more energy-efficient amine regeneration. From a thermodynamics point of view, the change in regeneration enthalpy decreased in the case of these non-aqueous solutions, suggesting less energy consumption in this case. Also, in this case, the reduction in activation energies will allow for running the desorption columns at much lower temperatures. This could enable us to completely rely on waste thermal energy instead of using expensive high-grade electrical heat energy. Although these results are very promising, other factors such as the solvent volatility should be also considered.

SUPPLEMENTARY MATERIAL

The supplementary material is available and contains activation energies (Table S1) and Gibbs free energies (Table S2) of the different forward and backward reactions. These tables compare the values obtained purely from DFT calculations to those obtained by combining coupled-cluster electronic energies and DFT vibrational frequency calculations. Table S3 reports the evaluation of including the dispersion and geometrical counterpoise corrections.

ACKNOWLEDGMENTS

This research was funded by EPSRC (Grant No. EP/N024672/1).

AUTHOR DECLARATIONS

Conflict of Interest

The authors have no conflicts to disclose.

Author Contributions

N. D. Afify: Writing – original draft (equal); Writing – review & editing (equal). **M. B. Sweatman:** Supervision (equal); Writing – review & editing (equal).

DATA AVAILABILITY

The data used to support the findings of this study are included within the article. Should further data or information be required, these are available from the corresponding author upon request.

REFERENCES

- ¹Z. Henry Liang, W. Rongwong, H. Liu, K. Fu, H. Gao, F. R. Zhang Cao, T. Sema, A. Henni, K. Sumon, D. Nath, D. Gelowitz, W. Srisang, C. Saiwan, A. Benamor, M. Al Marri, H. Shi, T. Supap, C. Chan, Q. Zhou, M. Abu-Zahra, M. Wilson, W. Olson, R. Idem, and P. Tontiwachwuthikul, *Int. J. Greenhouse Gas Control* **40**, 26–54 (2015).
- ²S. J. McGurk, C. F. Martín, S. Brandani, M. B. Sweatman, and X. Fan, *Appl. Energy* **192**, 126–133 (2017).
- ³G. T. Rochelle, *Science* **325**, 1652–1654 (2009).
- ⁴K. Z. House, C. F. Harvey, M. J. Aziz, and D. P. Schrag, *Energy Environ. Sci.* **2**, 193 (2009).
- ⁵J. Husebye, A. L. Brunsvold, S. Roussanaly, and X. Zhang, *Energy Procedia* **23**, 381–390 (2012).
- ⁶B. Dutcher, M. Fan, and A. G. Russell, *ACS Appl. Mater. Interfaces* **7**, 2137–2148 (2015).
- ⁷C.-H. Yu, C.-H. Huang, and C.-S. Tan, *Aerosol Air Qual. Res.* **12**, 745–769 (2012).
- ⁸F. Bougie, D. Pokras, and X. Fan, *Int. J. Greenhouse Gas Control* **86**, 34–42 (2019).
- ⁹N. D. Afify and M. B. Sweatman, *J. Chem. Phys.* **148**, 204513 (2018).
- ¹⁰N. D. Afify and M. B. Sweatman, *J. Chem. Phys.* **148**, 024508 (2018).
- ¹¹F. Bougie and X. Fan, *Int. J. Greenhouse Gas Control* **79**, 165–172 (2018).
- ¹²N. D. Afify and M. B. Sweatman, *J. Chem. Phys.* **151**, 024503 (2019).
- ¹³G. Rochelle, E. Chen, S. Freeman, D. Van Wagener, Q. Xu, and A. Voice, *Chem. Eng. J.* **171**, 725–733 (2011).
- ¹⁴S. Martin, H. Lepaumier, D. Picq, J. Kittel, T. de Bruin, A. Faraj, and P.-L. Carrette, *Ind. Eng. Chem. Res.* **51**, 6283–6289 (2012).
- ¹⁵A. Hartono, A. F. Cifija, P. Brúder, and H. F. Svendsen, *Energy Procedia* **63**, 2138–2143 (2014).
- ¹⁶E. Gjernes, L. I. Helgesen, and Y. Maree, *Energy Procedia* **37**, 735–742 (2013).
- ¹⁷F. Closmann, T. Nguyen, and G. T. Rochelle, *Energy Procedia* **1**, 1351–1357 (2009).
- ¹⁸F. Bougie and M. C. Iliuta, *Ind. Eng. Chem. Res.* **49**, 1150–1159 (2010).
- ¹⁹B. Zhao, Y. Sun, Y. Yuan, J. Gao, S. Wang, Y. Zhuo, and C. Chen, *Energy Procedia* **4**, 93–100 (2011).
- ²⁰S.-W. Park, J.-W. Lee, B.-S. Choi, and J.-W. Lee, *Korean J. Chem. Eng.* **23**, 806–811 (2006).

- ²¹N. El Hadri, D. V. Quang, E. L. V. Goetheer, and M. R. M. Abu Zahra, *Appl. Energy* **185**, 1433–1449 (2017).
- ²²M. Lail, J. Tanhana, and L. Coleman, *Energy Procedia* **63**, 580–594 (2014).
- ²³M. Tao, J. Gao, P. Zhang, W. Zhang, Q. Liu, Y. He, and Y. Shi, *Energy Fuels* **31**, 6298–6304 (2017).
- ²⁴F. J. Tamajón, E. Álvarez, F. Cerdeira, and D. Gómez-Díaz, *Chem. Eng. J.* **283**, 1069–1080 (2016).
- ²⁵P. M. Matthias, F. Zheng, D. J. Heldebrant, A. Zwoster, G. Whyatt, C. M. Freeman, M. D. Bearden, and P. Koech, *ChemSusChem* **8**, 3617–3625 (2015).
- ²⁶M. Hasib-ur-Rahman and F. Larachi, *Environ. Sci. Technol.* **46**, 11443–11450 (2012).
- ²⁷R. Hart, P. Pollet, D. J. Hahne, E. John, V. Llopis-Mestre, V. Blasucci, H. Hutenhower, W. Leitner, C. A. Eckert, and C. L. Liotta, *Tetrahedron* **66**, 1082–1090 (2010).
- ²⁸M. Cui, S. Chen, T. Qi, and Y. Zhang, *J. Chem. Eng. Data* **63**, 1198–1205 (2018).
- ²⁹F. Barzagli, S. Lai, and F. Mani, *Energy Procedia* **63**, 1795–1804 (2014).
- ³⁰F. Barzagli, F. Mani, and M. Peruzzini, *Int. J. Greenhouse Gas Control* **16**, 217–223 (2013).
- ³¹M. J. Frisch, G. W. Trucks, H. B. Schlegel, G. E. Scuseria, M. A. Robb, J. R. Cheeseman, G. Scalmani *et al.*, Gaussian 16, Rev. C 01, 2016.
- ³²G. M. J. Barca, C. Bertoni, L. Carrington, D. Datta, N. De Silva, J. E. Deustua, D. G. Fedorov, J. R. Gour *et al.*, *J. Chem. Phys.* **152**, 154102 (2020).
- ³³F. Neese, F. Wennmohs, U. Becker, and C. Riplinger, *J. Chem. Phys.* **152**, 224108 (2020).
- ³⁴M. G. Evans and M. Polanyi, *Trans. Faraday Soc.* **31**, 875–894 (1935); H. Eyring, *Trans. Faraday Soc.* **3**(2), 107–115 (1935).
- ³⁵V. Barone and M. Cossi, *J. Phys. Chem. A* **102**, 1995–2001 (1998).
- ³⁶T. Davran-Candan, *J. Phys. Chem. A* **118**, 4582–4590 (2014).
- ³⁷S. Gangarapu, A. T. M. Marcelis, Y. A. Alhamed, and H. Zuilhof, *ChemPhysChem* **16**, 3000–3006 (2015).
- ³⁸E. Orestes, C. Machado Ronconi, and J. W. D. M. Carneiro, *Phys. Chem. Chem. Phys.* **16**, 17213–17219 (2014).
- ³⁹H.-B. Xie, Y. Zhou, Y. Zhang, and J. K. Johnson, *J. Phys. Chem. A* **114**, 11844–11852 (2010).
- ⁴⁰K. Z. Sumon, C. H. Bains, D. J. Markewich, A. Henni, and A. L. L. East, *J. Phys. Chem. B* **119**, 12256–12264 (2015).
- ⁴¹H. M. Stowe and G. S. Hwang, *Ind. Eng. Chem. Res.* **56**, 6887–6899 (2017).
- ⁴²T. Zhang, Y. Yu, and Z. Zhang, *Mol. Simul.* **44**, 815–825 (2018).
- ⁴³S. Kim, H. Shi, and J. Y. Lee, *Int. J. Greenhouse Gas Control* **45**, 181–188 (2016).
- ⁴⁴B. Han, C. Zhou, J. Wu, D. J. Tempel, and H. Cheng, *J. Phys. Chem. Lett.* **2**, 522–526 (2011).
- ⁴⁵Y. Matsuzaki, H. Yamada, F. A. Chowdhury, T. Higashii, S. Kazama, and M. Onoda, *Energy Procedia* **37**, 400–406 (2013).
- ⁴⁶Y. Matsuzaki, H. Yamada, F. A. Chowdhury, T. Higashii, and M. Onoda, *J. Phys. Chem. A* **117**, 9274–9281 (2013).
- ⁴⁷I. Sandler, J. Chen, M. Taylor, S. Sharma, and J. Ho, “Accuracy of DLPNO-CCSD(T): Effect of basis set and system size,” *J. Phys. Chem. A* **125**(7), 1553–1563 (2021).
- ⁴⁸L. Goerigk, A. Hansen, C. Bauer, S. Ehrlich, A. Najibi, and S. Grimme, “A look at the density functional theory zoo with the advanced GMTKN55 database for general main group thermochemistry, kinetics and noncovalent interactions,” *Phys. Chem. Chem. Phys.* **19**(48), 32184–32215 (2017).
- ⁴⁹H. Kruse and S. Grimme, “A geometrical correction for the inter- and intra-molecular basis set superposition error in Hartree–Fock and density functional theory calculations for large systems,” *J. Chem. Phys.* **136**(15), 154101 (2012).
- ⁵⁰S. Grimme, S. Ehrlich, and L. Goerigk, “Effect of the damping function in dispersion corrected density functional theory,” *J. Comput. Chem.* **32**(7), 1456–1465 (2011).
- ⁵¹S. H. Ali, *Int. J. Chem. Kinet.* **37**, 391–405 (2005).
- ⁵²E. Alper, *Ind. Eng. Chem. Res.* **29**, 1725–1728 (1990).
- ⁵³S. Xu, Y.-W. Wang, F. D. Otto, and A. E. Mather, *Chem. Eng. Sci.* **51**, 841–850 (1996).
- ⁵⁴G. Bruhn, E. R. Davidson, I. Mayer, and A. E. Clark, *Int. J. Quantum Chem.* **106**, 2065–2072 (2006).